Dual-Segment Three-phase PMSM with Dual Inverters for Leakage Current and Common-mode EMI Reduction

Zewei Shen, *Student Member*, *IEEE*, Dong Jiang, *Senior Member*, *IEEE*, Tianjie Zou, *Student Member*, *IEEE*, Ronghai Qu, *Fellow*, *IEEE*

***Abstract*—In motor drive system, the inverter working in discrete and impulse state generate the common mode voltage (CMV) in the terminal of stator winding neutral point. The high frequency CMV can induce the leakage current and common-mode (CM) electromagnetic interference (EMI) which is a potential threat to personal safety and system stability. The conventional single three-phase inverter is proved powerless to eliminate the CMV, while the two paralleled inverters can effectively eliminate the CMV theoretically, but the three coupled inductors (CIs) should be added in the motor drive system which reduces the power density and efficiency of the system. A novel method which associates the special designed dual-segment three-phase motor with the CMV elimination modulation algorithm can be utilized to cancel the extra CIs without degrading the function of leakage current and CM EMI suppression. Design of the dual-segment three-phase PMSM is introduced, with the identical back-EMFs for two groups of windings but little magnetic coupling between them. Simulation and experimental results are provided to verify the validity of proposed method in CM related reduction and CI cancellation. Compared with previous work of zero-CM PWM for paralleled inverters, the proposed dual-segment three-phase motor drive can achieve better power density by removing the coupled inductors.**

***Index Terms*—common mode, electromagnetic interference, coupled inductors, dual-segment three-phase machine**

Acronym in this paper:

PWM: Pulse Width Modulation

VSI: Voltage Source Inverter

CMV: Common-mode Voltage

CMC: Common-mode Current

CI: Coupled Inductor

EMI: Electromagnetic Interference

IPM: Integrated Power Module

ASD: Adjustable Speed Drive

I. INTRODUCTION

In recent years, voltage source inverters (VSIs) with pulse width modulation (PWM) are widely used in adjustable speed drive (ASD) occasions due to various advantages, such as high efficiency, superior dynamic performance, low harmonic distortion. Despite the above merits, with the discrete characteristic of output voltage for VSI, some drawbacks are generated, including high switching losses in high switching frequency occasion, high frequency torque ripple caused by the switching current, and one of the most concerned drawbacks is the common mode voltage (CMV) which induces a series of problems, such as grounding leakage current, common mode (CM) electromagnetic interference (EMI), shaft voltage and bearing current [1]–[4].

Based on the principle of the CMV related problems, some typical methods can be utilized to restrain them correspondingly. For example, the grounding leakage current can be suppressed by inserting the CM choke between the inverter and the motor[5]-[7], the CM EMI can be mitigated by the passive, active or hybrid CM EMI filters [8]-[10], and the bearing current can be reduced utilizing insulated bearing [11]. Though these methods can be implemented, the CM choke and CM EMI filter bring more weight and complexity for the system, and the insulated bearing comes with significant penalty on cost. In addition, these solutions only deal with one particular problem at a time, more simplified and universal method to solve all the CMV related problems should be considered.

Since the CMV which is the combination of whole pole voltages for VSI generates the motor related problems, the simple and universal approach is to restrain the CMV based on the modification of modulation algorithm. For example, in two-level three-phase VSI, AZSPWM (active zero state PWM) and NSPWM (near state PWM) schemes can be deduced from the typical SVPWM (space vector PWM) and DPWM (discontinuous PWM) schemes correspondingly which both avoid the usage of zero voltage vectors [12]-[14], so that maximum CMV amplitude can be reduced. But with the limitation of switching states flexibility and odd number phase-legs, conventional two-level three-phase VSI can only reduce the CMV but cannot eliminated it, which leads the CM EMI filter inevitable for the motor drive system. To deal with the problem of insufficient freedom, the modified topology can be utilized to realize CMV elimination effect. In [15][16], the three-level and multilevel inverters cooperating with particular PWM schemes can be utilized to eliminate the CMV in typical three-phase load, but with the tradeoff of the current ripple and THD deterioration. In [17], the dual-winding stator configuration driven by dual inverter which provides even switching states combination is implemented for CMV cancellation, and the simplified

Manuscript received Jun 05, 2018; revised Aug 09, 2018; accept Aug 09, 2018. This work was supported by the National Natural Science Foundation of China under Project 51607077 (Corresponding author: Dong Jiang)Zewei Shen, Dong Jiang, Tianjie Zou and Ronghai Qu are with State Key Laboratory of Advanced Electromagnetic Engineering and Technology, School of Electrical and Electronic Engineering, Huazhong University of Science and Technology, Wuhan 430074, China (e-mail: shenzw@hust.edu.cn, jiangd@hust.edu.cn, txwj129@hust.edu.cn ronghaiqu@hust.edu.cn).

structure with nine-switch inverter had been proved to retain the similar CMV elimination effect [18] [19].

Similarly, the dual inverter with paralleled manner is a popular structure which not only has the ability to increase the power rating of the system [20], but also has the possibility to suppress or even eliminate the CMV in idea condition [21][22]. The system configuration of paralleled inverters fed three phase AC motor is shown in Fig. 1. The paralleled manner realization is contributed to the three extra coupled inductors (CIs) which limit the circulating current for paralleled phase-legs. Compared to other CMV elimination schemes' topology [15]-[19], though the proposed ZCMV PWM scheme in [22] has the potential to cancel out the big CM choke, the added three CIs not only increase the volume and weight for the system, but also make the whole system complex. Meanwhile, in large power application, the DC bus voltage is usually high and the switching frequency is often limited to hundreds Hz or several kHz which obviously enlarge the circulating current [23] and leads to design and manufacture huge CI that loses the superiority of CM choke cancellation effect or may reduce the power density of the system finally.

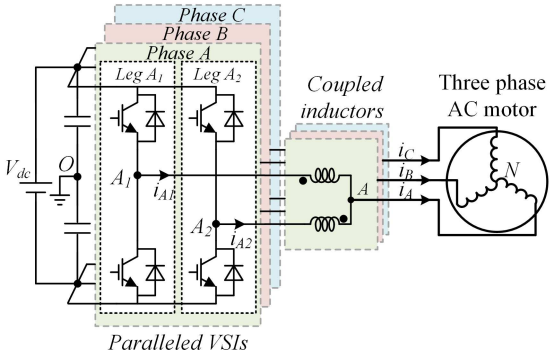

Fig. 1. System configuration of paralleled inverters fed three phase AC motor with coupled inductors

The pivotal role of CI is providing the suitable inductance in the circulating path to restrain the circulating current. Actually, there exists the other kind of inductor in the ASD system, *i.e.* the stator inductor of motor, which has the potential to offer the so called "suitable inductance". In order to make the stator inductor integrated with the function of circulating current suppression, the special motor should be designed to work in with dual inverter. In this condition, the motor ASD system can be consisted of dual inverter and the special designed motor without the extra CIs which not only simplify the ASD system, but also increase the power density of whole system. This paper will give the detailed introduction of overall method for ZCMV scheme with the special designed motor to realize the CMV related problem mitigation.

The rest of this paper is organized as follows: with the analysis of different CMV reduction modulation schemes, the principle of CI elimination is introduced with theoretical analysis in part II. To satisfy the demand of the stator winding and back-EMF to cooperate with the selected ZCMV scheme, the special dual-segment three-phase permanent magnet synchronous machine (PMSM) is introduced in part III, which includes the design result, approximate mathematical model and corresponding control strategy. In part IV, the proposed structure utilized ZCMV method is firstly tested and compared with other schemes by simulation, especially make fair and detailed comparison with the already proposed paralleled inverter with CI scheme. The detailed experimental results are presented in part V to prove the proposed method's validity and superiority. Conclusions are summarized in part VI finally.

II. THE STRUCTURE OPTIMIZATION OF MOTOR DRIVE SYSTEM

A. The Analysis of Different CMV Reduction Modulation Schemes

Based on the system structure shown in Fig. 1, the simplified equivalent circuit model of the system can be set up and shown in Fig. 2, where V_{A1O}, V_{A2O}, V_{B1O}, V_{B2O}, V_{C1O} and V_{C2O} are the pole voltages of six phase-legs which switch between the value of $\pm V_{dc}/2$ with the DC link voltage of V_{dc}, i_{A1}, i_{A2}, i_{B1}, i_{B2}, i_{C1} and i_{C2} are the phase-leg currents, i_A, i_B and i_C are the output phase currents, i_{Ac}, i_{Bc} and i_{Cc} are the three phase circulating currents flowing through CIs correspondingly. For each CI, L_c, M and R_c are the main inductance, mutual inductance and resistance correspondingly. As for the three-phase motor, each phase can be simplified as a stator inductor, a stator resistance and a back electromotive force (EMF) with series connection which are represented by L_S, R_S, e_X (X=A, B, C) correspondingly.

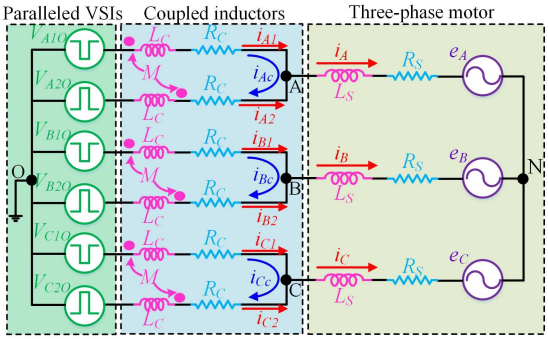

Fig. 2 Simplified equivalent circuit model of paralleled inverters system with three phase motor

Considering the symmetry of CI, the phase voltage (taking the DC side middle point as reference) can be deduced with the principle of circuit simplification and shown in (1).

$$V_{XO} = \frac{1}{2}\left(V_{X1O} + V_{X2O}\right), \quad (X = A, B, C) \qquad (1)$$

In this case, when paralleled phase-legs output the same pole voltages, whether $V_{dc}/2$ or $-V_{dc}/2$, the combined output phase voltage of CI keep the identical states. When paralleled phase-legs output the opposite pole voltages, the combined output phase voltage of CI is zero and the circulating current obviously vary in this condition. So the essence of paralleled inverters with CIs is the three-level inverter and the critical role of CI is providing the function of different switching state combination.

In addition, with the symmetry of motor stator windings, the CMV in the conventional three-phase motor can be deduced which is the instantaneous average value of three phase voltages. In consequence, the CMV generated by the paralleled inverters is

$$V_{cm}=\frac{1}{3}(V_{AO}+V_{BO}+V_{CO})$$
$$=\frac{1}{3}\left[\frac{1}{2}(V_{A1O}+V_{A2O})+\frac{1}{2}(V_{B1O}+V_{B2O})+\frac{1}{2}(V_{C1O}+V_{C2O})\right]$$
$$=\frac{1}{6}(V_{A1O}+V_{A2O}+V_{B1O}+V_{B2O}+V_{C1O}+V_{C2O}) \quad (2)$$

With the number of phase-legs increased to six, the more combinatorial CMV values can be realized, especially the zero state which cannot be occurred in single three-phase inverter driven system.

In order to restrain the circulating current and reduce the volume of CI in paralleled inverters, the high-frequency technology should be implemented which demands the paralleled phase-legs keeping the identical average pole voltage in every switching cycle. To satisfy the above requirement, [22] has introduced three different modulation schemes, including conventional SVPWM, SVPWM with half switching cycle interleaving and ZCMV schemes, which the effects of CMV reduction are different. The basic principle of reference voltage synthesis for SVPWM is shown in Fig. 3(a). In conventional SVPWM scheme, the corresponding phase-legs are driven by identical PWM signals which leads to the identical currents for paralleled phase-legs in ideal condition. In this case, the phase voltage only switches between $V_{dc}/2$ and $-V_{dc}/2$. In addition, because of the same zero voltage vectors (000,111) utilized simultaneously, the CMV has maximum peak value of $\pm V_{dc}/2$ shown in Fig .3(b). In order to reduce the CMV, the extra interleaving strategy for paralleled inverters can be utilized shown in Fig .3(c). With half switching cycle interleaving, the voltage vectors' combination can be changed. More importantly, the CMV can be reduced to $\pm V_{dc}/6$ with the effect of canceling out different zero voltage vectors. But only interleaving manner cannot eliminate the CMV, the impairment of motor caused by CMV still exists.

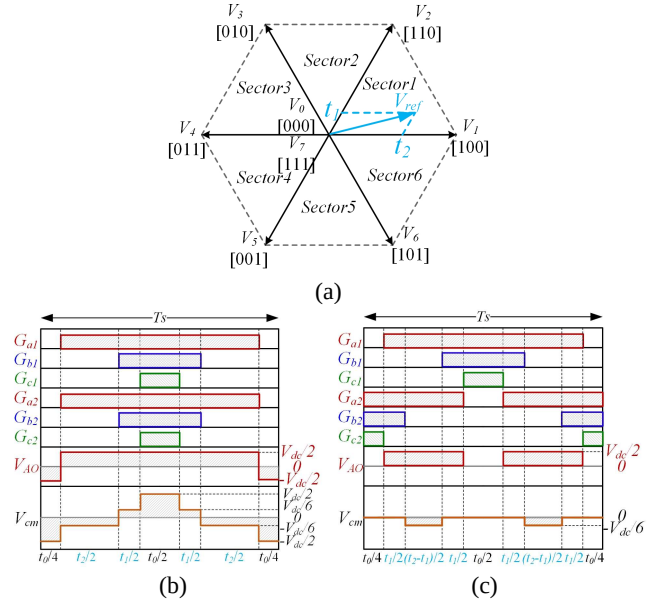

Fig. 3 The conventional modulation schemes for paralleled inverters: (a) the principle of reference voltage synthesis with space voltage vectors for SVPWM, (b) the conventional SVPWM scheme, (c) the SVPWM with half switching cycle interleaving scheme

Fig .4 shows the characteristic of ZCMV scheme, including the sector division and PWM signals distribution. In Fig .4(a), it can be found that the sector division of ZCMV has thirty degree lag comparing to SVPWM and the six active voltage vectors are made up of basic adjacent voltage vectors. In each sector, the reference voltage can be generated by two adjacent active paralleled voltage vectors with common paralleled zero voltage vectors. The principle of reference voltage vector synthesis is similar with SVPWM which the active times for two adjacent paralleled voltage vectors are t_1 and t_2 in each switching cycle, with the remaining zero vector time of t_0. The PWM signals, phase voltage and CMV in sector 1 are depicted in Fig .4(b). It can be seen that the PWM signals of phase B and C are artificially changed asymmetric to make each rising edges and falling edges aligned which can eliminate the instantaneous CMV pulse and keep the CMV zero in whole switching cycle. So the ZCMV scheme has best CMV suppression effect theoretically. The more detailed principle for this novel modulation scheme can be found in [22].

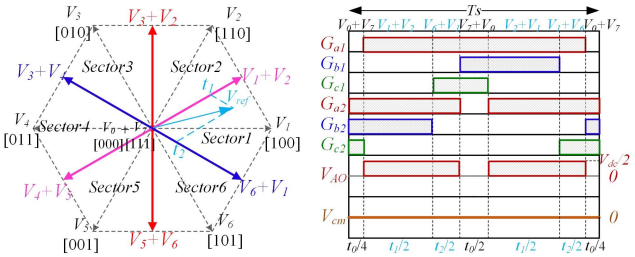

Fig. 4 The principle of ZCMV scheme for paralleled inverters: (a) the reference voltage synthesis, (b) PWM scheme in sector 1

Though [22] has introduced the ZCMV scheme, the CMV suppression effects are only tested with R-L load, not the most concerned object-AC motor. More importantly, the modulation scheme is only suitable for paralleled inverters and the three bulky CIs are inevitably utilized which leads to the system more complex than other CMV elimination schemes, like the three-level CMV elimination scheme directly driving three-phase motor [15] and dual-inverter driving dual three-phase winding motor [17]. In view of the two problems mentioned above, in the following content, the principle of CI elimination is introduced which makes the requirement of motor explicitly, and the test of ZCMV scheme with the special designed motor is implemented to verify the feasibility and superiority comparing to the conventional paralleled inverters with CIs scheme.

B. The principle of coupled inductor elimination

In order to deduce the principle of CI elimination and simplify the analysis, two paralleled phase-legs with single CI and the corresponding phase load are extracted. Taking phase A for example, the single-phase model can be built and shown in Fig. 5(a). It can be seen that both the CI and phase load have inductors. The main inductor of CI is to limit the circulating current between the paralleled phase-legs caused by the instantaneous pole voltage difference, while the inductor of phase load is the stator inductor of motor. If this two inductors can be integrated to one inductor, the simplified system which eliminates coupled inductors can be realized.

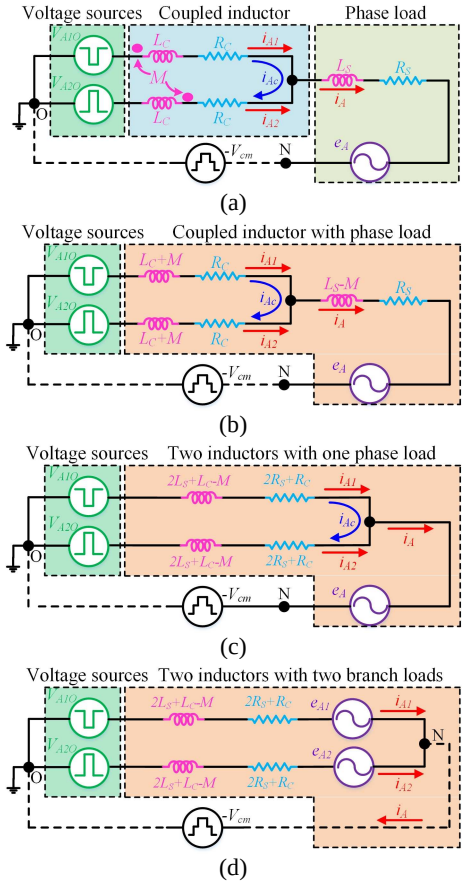

Fig. 5 The process of coupled inductor elimination: (a) the original equivalent circuit model of one phase, (b) the equivalent circuit model with coupled inductor decoupling, (c) the equivalent circuit model with merging of external inductors and stator inductor, (d) the equivalent circuit model without external inductors

Following the above idea, Fig. 5(b)-(d) shows the simplified process. By utilizing the circuit decoupling equivalence principle, Fig. 5(b) depicts the equivalent circuit with the CI decoupling. In this condition, the two inductors L_c+M can be regarded as two external separate inductors inserted into the circulating path to limit the circulating current i_{Ac}, while the inductor L_S-M can be regarded as new motor stator inductor. Based on the circuit principle of series and parallel transformation, the equivalent circuit model in Fig. 5(b) can be further simplified, and the result is shown in Fig. 5(c). Under this circumstance, the external inductor and the stator inductor can be merged to one inductor with the inductance of $2L_S+L_c$-M, and the merged resistance follows the same law with the value of $2R_S+R_c$. In this case, the combined inductor not only provides the function of circulating current suppression, but also can be regarded as the stator inductor, so the external inductor can be eliminated. Meanwhile, considering the mandatory rule that one stator inductor should have its own back EMF, the back EMF of one phase should be decomposed into two back EMFs and the phase load can be regarded as two branch loads shown in Fig. 5(d). The increasing number of stator inductor means the physical changing requirement of motor that one set stator winding should increase to two, so the conventional three-phase motor should be modified to dual three-phase winding motor. In addition, according to the circuit principle, the relationship $e_{A1}=e_{A2}=e_A$ should be satisfied, so each homologous two stator inductors should have identical back EMF. It should be clarified that though the winding configuration are similar comparing to the methods proposed in [17]-[19], the back EMF demand of homologous two stator inductors are different which eventually make the modulation algorithm distinct.

Considering the definition of CMV for this special motor, the CMV keeps unchanged comparing to formula (2), while the influence of stator winding modification for the CMV related problem should be analyzed. In conventional three-phase motor with single set stator winding, taking the main impedance of CM path in the motor into consideration, the simplified CM equivalent model can be drawn and shown in Fig. 6(a), where Z_{dg} is the dc-link midpoint grounding impedance, Z_{cable} is the transmission impedance of cable for each phase. C_{sf} and C_{sr} are the capacitor between stator winding and motor frame, stator winding and rotor for each phase, and C_{rf} represent the entire capacitive coupling between rotor and motor frame [3]. It should be noted that the high frequency leakage current is not a conduction current flowing in the stator winding, but a displacement current caused by the corresponding stray capacitors [1]. So R_{sf}, R_{sr} and R_{rf} are not the conductive resistances but express the iron core loss for the high frequency leakage current physically [24]. The simplified model for the motor bearing consists of the resistor R_b, the switch S_b and adjustable capacitor C_b [3]. Owing to the symmetric characteristic of the CM equivalent branch circuit for each phase in ideal condition, it can be easily deduced that the induced motor frame voltage can be restrained to zero with the ZCMV modulation scheme, so the leakage current and CM EMI can also be suppressed.

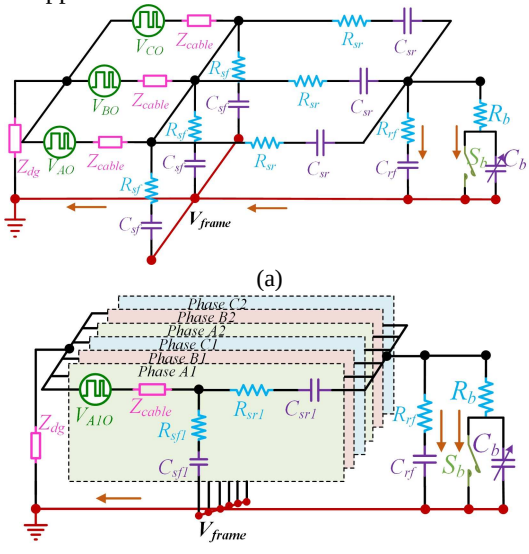

Fig. 6 The CM equivalent model comparison for typical three-phase motor drive system and the dual-three-phase motor drive system: (a) the typical three-phase motor drive system, (b) the dual-three-phase motor drive system

Similarly, considering the stray coupling in dual winding motor, the corresponding CM equivalent model can also be set up and shown in Fig. 6(b). With the number of stator winding increased, the parasitic coupling branch of the stator winding should also be increased and the corresponding stray parameters which decide by the coupling area for each phase

winding should be changed. So the impedance between stator winding and motor frame, the impedance between stator winding and rotor are redefined as C_{sf1}, C_{sr1}, R_{sf1} and R_{sr1} correspondingly. As for the impedance between the rotor and frame, and the bearing model, they are not influenced by stator winding separation and keep the same. In this condition, with the symmetric characteristic of CM circuit, the high frequency displacement current can cancel out each other regardless of the increase of parasitic coupling branch, so the leakage current and CM EMI suppression effect can also be retained in ideal condition.

III. DUAL-SEGMENT THREE-PHASE PM MACHINE DESIGN AND CONTROL PRINCIPLE

Since the structure of the requested motor is more complicated than conventional three-phase PMSM, the design and control method should be considered. In this part, the proposed dual-segment three-phase motor design and back-EMF test is firstly implemented; then the simplified mathematical model of the designed motor is derivate; in addition, the relevant sector judging method for the ZCMV scheme is introduced, and the corresponding control block diagram is deduced based on the above analysis finally.

A. The dual-segment three-phase motor design and test

In order to build the motor drive system, a PMSM prototype with two sets of symmetrical three-phase windings has been designed. As shown in Fig. 7, the motor is constructed with a 12-slot stator wound with double-layer non-overlapping coils. The 8-pole pair PM rotor constitutes a slot/pole combination of 12/16 together with the stator. According to classical winding theory of AC machines, the periodicity number of the 12/16 motor is 4.

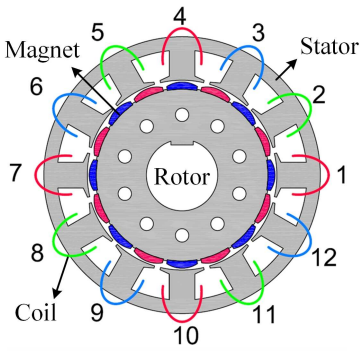

Fig. 7 Sketch of the motor topology

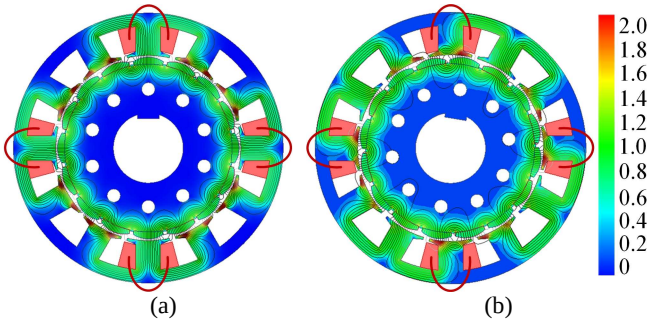

Fig. 8 Flux contour plots of the machine: (a) Open circuit, (b) Rated load

Fig. 8 gives the FEA-based flux contour plots of the motor under open circuit and rated load condition, and it can be clearly seen that the flux distribution repeats itself 4 times along the periphery. Due to this periodicity, the coils can be divided into 3 groups according to their difference in space vector, which are shifted by 120° electrical angle. Meanwhile, the 4 coils in each group can induce back-EMF with exactly the same waveform. Hence, one set of the dual-segment three-phase winding can be simply designed by selecting any 2 coils from each of group to form one phase. Practically, the dual-segment three-phase winding is implemented according to the star of slots plot shown in Fig. 9, and the winding is specifically configured as illustrated in Fig. 10. In order to investigate the mutual coupling of corresponding phases from each set of winding with the same back-EMF, the armature reaction of the motor is further evaluated through FEA. As illustrated in Fig. 11, there is only weak coupling between phase A1 and A2. Besides, the FEA-based calculation results show that mutual-inductance between A1 and A2 is only 0.1372mH, *i.e.*, ~11% that of the self-inductance of 1.172mH. So this special designed motor can prevent the stator inductor from being overly weakened by the mutual-inductance of different windings, which is favorable to restrain the increase of current ripple in phase-leg current.

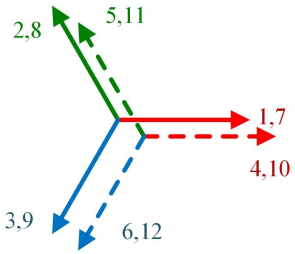

Fig. 9 Star of slots' vector gram.

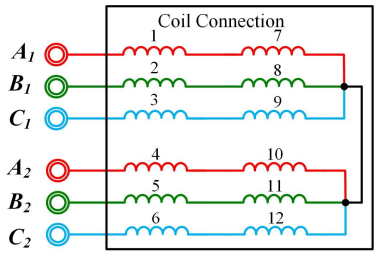

Fig. 10 Connection of two-segment windings.

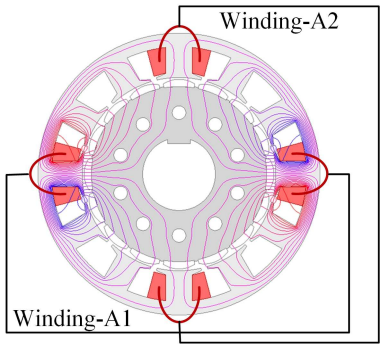

Fig. 11 Armature reaction of the winding A1.

According to classical winding theory of AC machines, the periodicity number of the 12/16 motor is 4. According to the optimal designed PMSM scheme, a two segments prototype PMSM has been fabricated. The stator, rotor and the assembled motor with the test bench are shown in Fig. 12(a) and Fig. 12(b). The two-segment rotor skewing is considered to optimize the output torque and reduce the cogging torque.

In addition, the key parameters of the designed PMSM are listed and shown in Table. I.

TABLE I. KEY PARAMETERS OF THE DEIGNED PMSM

Parameters	Value
PM flux linkage	0.023Wb
stator inductance	1.2mH
Phase resistance	0.2Ω
Rated rotation speed	1000rpm
Rated fundamental frequency	133.3Hz
Rated line voltage	75V
Rated line current	8.5A
Rated torque	8.3Nm

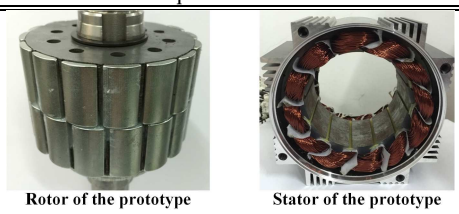

(a)

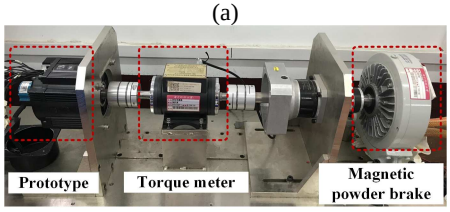

(b)

Fig. 12 The motor prototype and test bench: (a) the motor prototype, (b) the test bench

In order to verify the feasibility of the designed motor, the back-EMF test is firstly implemented in rated rotation speed. The results are shown in Fig. 13(a) and Fig. 13(b). It can be seen that fundamental electrical period of the back-EMF is 7.5ms which conforms to the design rated speed. More importantly, the homologous two stator inductors are proved to have nearly identical back-EMF. Considering the fundamental and harmonic voltages in the back-EMF, the frequency domain analysis is implemented, it can be seen that the fundamental back-EMF of all stator inductors are close to 33V, and the harmonics are small enough to be ignored in motor control process.

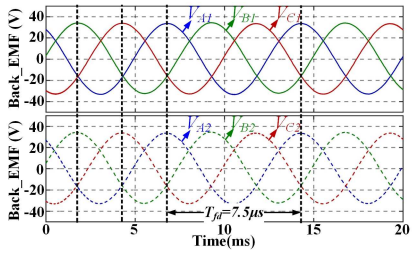

(a)

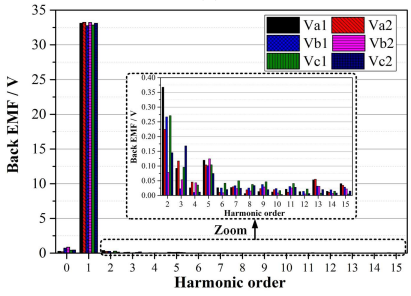

(b)

Fig. 13 The tested result of back-EMF for dual-segment motor: (a) the time domain waveform, (b) the frequency domain analysis

B. The mathematical model for the dual-segment three-phase motor

For general dual three-phase motor, it often consists of two sets three-phase windings spatially shifted by thirty electrical degrees. In addition, the two sets stator winding have obvious magnetic coupling which adds the complexity of mathematic model for dual three-phase motor, and also leads to the complexity of control method. Contrary, though the designed dual-segment motor have multi-set stator windings, the stator winding sets only exist three phase back-EMF. More importantly, under the FEA analysis, different set phase windings with the same back EMF have little magnetic coupling, so the influence of different stator winding sets can be neglected to reduce the complexity of the system. In this case, the modeling of the designed motor can be regard as the combination of two conventional three-phase motors, and the control method can follows the conventional three-phase AC motor's control method. So ignoring the small magnetic coupling between the two set of windings, the mathematical model of each set winding is identical with regular three-phase PM machine, and the flux and voltage equations in the d-q reference frame can be written as (3) and (4)

$$\begin{bmatrix}\psi_{d1}\\ \psi_{q1}\\ \psi_{d2}\\ \psi_{q2}\end{bmatrix}=\begin{bmatrix}L_{d1}&0&0&0\\ 0&L_{q1}&0&0\\ 0&0&L_{d2}&0\\ 0&0&0&L_{q2}\end{bmatrix}\begin{bmatrix}i_{d1}\\ i_{q1}\\ i_{d2}\\ i_{q2}\end{bmatrix}+\begin{bmatrix}\psi_f\\ 0\\ \psi_f\\ 0\end{bmatrix} \tag{3}$$

$$\begin{bmatrix}U_{d1}\\ U_{q1}\\ U_{d2}\\ U_{q2}\end{bmatrix}=\begin{bmatrix}R_S&0&0&0\\ 0&R_S&0&0\\ 0&0&R_S&0\\ 0&0&0&R_S\end{bmatrix}\begin{bmatrix}i_{d1}\\ i_{q1}\\ i_{d2}\\ i_{q2}\end{bmatrix}+\frac{d}{dt}\begin{bmatrix}\psi_{d1}\\ \psi_{q1}\\ \psi_{d2}\\ \psi_{q2}\end{bmatrix}+\omega_r\begin{bmatrix}-\psi_{q1}\\ \psi_{d1}\\ -\psi_{q2}\\ \psi_{d2}\end{bmatrix} \tag{4}$$

where ψ_{dk}, ψ_{qk}, U_{dk}, U_{qk}, i_{dk}, i_{qk} (k=1, 2) are the d-q axis flux linkages, voltages, currents respectively. ψ_f is the flux linkage produced by permanent magnetics, R_S is the stator resistance per phase. ω_r stands for the electrical angular speed of the rotor. In this condition, the whole torque is composed of each segment torque of the motor. Considering the characteristic L_{dk}=L_{qk} in this surface-mounted PMSM, so the simplified equation for the total torque can be deduced and shown in (5).

$$\begin{aligned}T_e&=\frac{3}{2}p\left[\psi_f\left(i_{q1}+i_{q2}\right)+\left(L_{d1}-L_{q1}\right)i_{d1}i_{q1}+\left(L_{d2}-L_{q2}\right)i_{d2}i_{q2}\right]\\&=\frac{3}{2}p\psi_f\left(i_{q1}+i_{q2}\right)\end{aligned} \tag{5}$$

With above analysis, for the designed dual-segment three-phase motor, the output torque is decided by the summation of two q-axis current in each set stator winding. As for other aspect of the control process, it follows the conventional control principle and is similar to conventional three-phase motor.

C. The sector judging method of ZCMV modulation scheme

In close-loop control process, the key step is accurately judging the sector real-time. With the research of inherent

correlation between carrier-based PWM and conventional SVPWM in two-level inverter, the reduced computational method can be used to realize SVPWM effect without sector judgement, but for injecting the real-time CM (common mode) modulated signal into the sinusoidal modulation wave [25]. As for ZCMV scheme, the pivotal phase-shift process for PWM signals is decided by the sector [22]. However, whether the average or instantaneous CMV are eliminated, so the CM injection method cannot implemented in this case, and novel sector judging method should be developed.

For ZCMV scheme, the reference output average voltage of six phase-legs can be got from the d-q current controllers by inverse Park transform and listed as:

$$\begin{cases} V_{a1} = V_{a2} = d_a^* \cdot V_{dc} / 2 \\ V_{b1} = V_{b2} = d_b^* \cdot V_{dc} / 2 \\ V_{c1} = V_{c2} = d_c^* \cdot V_{dc} / 2 \end{cases} \tag{6}$$

where d_a^*, d_b^*, d_c^* are the quasi-duty cycle varying from -1 to 1. Considering the effect of CMV elimination effect for this scheme, the equation (7) can be deduced.

$$\begin{aligned} V_{\text{cm}} &= \frac{1}{6}\left(V_{A1O} + V_{A2O} + V_{B1O} + V_{B2O} + V_{C1O} + V_{C2O}\right) \\ &= \frac{V_{dc}}{3}\left(d_a^* + d_b^* + d_c^*\right) = 0 \end{aligned} \tag{7}$$

So the summation of three quasi-duty cycles must be zero in every switching cycle, and this potential constraint can be utilized to judge the sector. Actually, two quasi-duty cycles with the same sign can be used to determine the sector and all six combinations of the three quasi-duty cycles can uniquely determine six sectors. For example, when d_b^* and d_c^* are both negative, d_a^* must be positive and the sector is 1. At the same time, the synthesized voltage vector's effective time t_1, t_2 and left time t_0 can be calculated as:

$$\begin{cases} t_1 = -d_c^* \\ t_2 = -d_b^* \\ t_0 = 1 - d_a^* \end{cases} \tag{8}$$

With the time t_1, t_2 and t_0, the PWM signal of six phase-legs can be decided according to the modulation algorithm. Similar with the above analysis, the all sectors' judging condition and time segment calculation can be listed and shown in Table. II. According to the Table. II, the sector can be judged and the PWM signals in the whole fundamental period can be decided.

TABLE. II THE SECTOR JUDGING CONDITION AND TIME SEGMENT CALCULATION OF ZCMV PWM ALGORITHM

	Sector judging condition	Time segment calculation
sector 1	$d_b^* < 0, d_c^* < 0$	$t_1 = -d_c^*, t_2 = -d_b^*, t_0 = 1 - d_a^*$
sector 2	$d_a^* > 0, d_b^* > 0$	$t_1 = d_b^*, t_2 = d_a^*, t_0 = 1 + d_c^*$
sector 3	$d_a^* < 0, d_c^* < 0$	$t_1 = -d_a^*, t_2 = -d_c^*, t_0 = 1 - d_b^*$
sector 4	$d_b^* > 0, d_c^* > 0$	$t_1 = d_c^*, t_2 = d_b^*, t_0 = 1 + d_a^*$
sector 5	$d_a^* < 0, d_b^* < 0$	$t_1 = -d_b^*, t_2 = -d_a^*, t_0 = 1 - d_c^*$
sector 6	$d_a^* > 0, d_c^* > 0$	$t_1 = d_a^*, t_2 = d_c^*, t_0 = 1 + d_b^*$

With the aforementioned analysis, the control block diagram of the system can be set up and shown in Fig. 14. The control strategy is similar with normal field oriented control for three phase motor. The different part are the sector judging method and the modulation algorithm. In addition, the current feedback control which needs sampling six phase-legs' currents should combine the corresponding phase-legs' currents into one phase before adopting inverse Park and Clark transformation ($abc/\alpha\beta$ and $\alpha\beta/dq$).

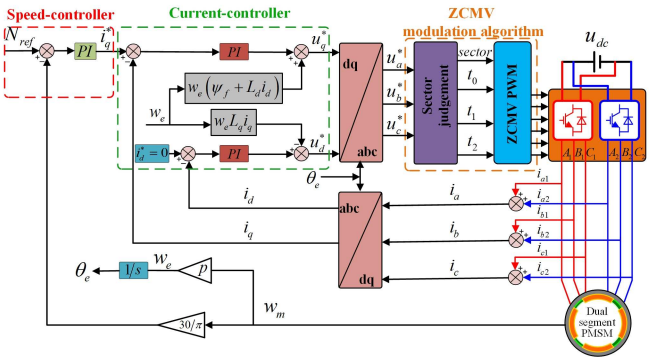

Fig. 14 The control block diagram of the system

IV. SIMULATION RESULTS

In order to test the effect of proposed dual-segment motor controlled by ZCMV scheme and make fair comparison with other methods, the simulation model based on Matlab/Simulink software has been conducted. Fig. 15 shows the different stator winding configurations of the dual-segment three-phase motor for different structures, in which the first configuration is based on paralleled inverters with CI structure shown in Fig. 15(a), while the other stator winding configuration is the proposed dual inverter with dual stator winding structure shown in Fig. 15(b).

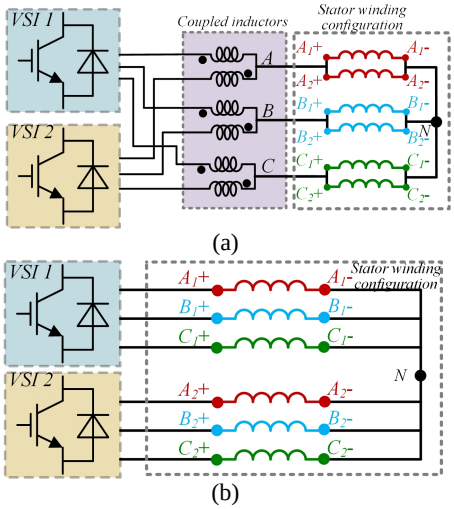

Fig. 15 The different stator winding configurations: (a) the paralleled inverters with CI, (b) the dual inverter with dual winding

Based on the designed parameters for the dual-segment three-phase motor, the suitable simulation parameters can be decided and shown in Table. III. Simulation is with DC link voltage of 75V and 10 kHz switching frequency. The main parameters for coupled inductor which include main inductance and coupling coefficient can be extracted from the actual CI to simulate the actual condition. What's more, the main CM loop which neglects the influence of bearing for the leakage current, *i.e.* the stray circuit between the stator winding and the motor frame is added in the

simulation model to test the characteristic of leakage current for different modulation schemes. The stray capacitor for each phase winding and motor frame can be extracted by LCR meter KEYSIGHT E4980AL, while the value of equivalent resistor is an estimated value which refer to the literature [1].

TABLE III. SIMULATION PARAMETERS

Symbol	Parameters	Value
V_{dc}	DC link voltage	75V
f_s	Switching frequency	10kHz
L_c	Main inductance of CI	0.52mH
M	Coupling coefficient of CI	0.92
L_s	Stator inductance	1.2mH
N_{ref}	Reference rotation speed	375rpm
f_0	Fundamental electrical frequency	50Hz
i_d	D-axis reference current	0
i_q	Q-axis reference current	8.5A
T_e	Reference torque	4.15Nm
C_{sf}	stray capacitor for each phase winding and motor frame	0.15nF
R_{sf}	equivalent resistor for each phase winding and motor frame	100Ω

A. Comparison the CM related quantities for different schemes

First, considering the proposed dual inverter with dual winding structure, the winding neutral point voltage, *i.e.* the CMV comparison for different modulation schemes are implemented and shown in Fig. 16. In Fig. 16(a), the dual stator windings driven by the conventional SVPWM method generates big CMV with the peak value of $\pm V_{dc}/2$. Without changing any switching edges for different phase-legs, the CMV of the proposed structure keeps identical waveform with single inverter, and the every step change of CMV can lead to the electrostatically induced current. Fig. 16(b) shows the CMV of SVPWM with half switching cycle interleaving, it can be found that the peak value of CMV reduce to $\pm V_{dc}/6$, this is owing to the interleaving manner which can cancel out the switching actions to a certain extent, while there still exists rising edges misaligned with falling edges which lead to the discharging and charging current generated asynchronously, so the leakage current cannot be avoided in this case. Fig. 16(c) shows the CMV of the proposed ZCMV scheme, it can be deduced that all the rising edges align with the corresponding falling edges to maintain the zero state of CMV which conforms to the theoretical analysis, so the discharging and charging current can cancel out each other and leads to the output leakage current eliminated in ideal condition. As for the original paralleled inverter with CI structure, the CMV waveforms for different modulation schemes [22] are also coincident with the corresponding results in the proposed dual winding structure, which proves that the proposed structure has no influence on the CMV, and the ZCMV scheme can eliminate the CMV in ideal condition which has the best CMV suppression effect comparing to other schemes.

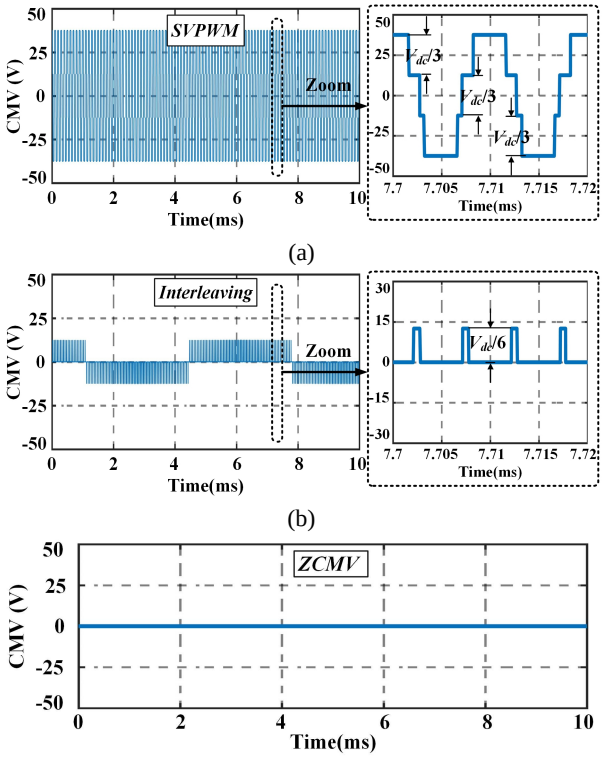

Fig. 16 The CMV comparison for different modulation schemes with the proposed structure: (a) the conventional SVPWM scheme, (b) the SVPWM with half switching cycle interleaving, (c) the proposed ZCMV scheme

In addition, the leakage current comparison of different schemes is also implemented. Fig. 17(a) shows the leakage current of conventional SVPWM scheme for the proposed structure. Without any different phase-legs' switching actions to cancel out the instantaneous *dv/dt*, the electrostatically induced leakage current generated and the six-step CMV induces six times leakage current in one switching cycle shown in the enlarge view. In addition, owing to relatively big step change of the CMV ($V_{dc}/3$) in every switching action, the peak vale of leakage current reaches nearly 0.2A in most cases. Fig. 17(b) shows the leakage current of SVPWM with half switching cycle interleaving scheme for the proposed structure. It can be found that the peak value of leakage current reduce to 0.1A which is attributed to the step change reduction of CMV ($V_{dc}/6$). Moreover, the generating times of leakage current in one switching cycle reduces from six to four shown in the enlarge view, this is caused by the left two CMV pulses' switching edges. Fig. 17(c) shows the proposed ZCMV scheme with the conventional and proposed structure. It can be clearly seen that the leakage current can be avoided in this two cases which is attributed to the every rising edges matching the corresponding falling edges to suppress the potential variation of motor frame, so the leakage current can be cancelled out finally. With the above analysis, it can be deduced that the proposed dual winding structure can maintain the effect of leakage current suppression and the ZCMV scheme has the best performance comparing to other modulation schemes.

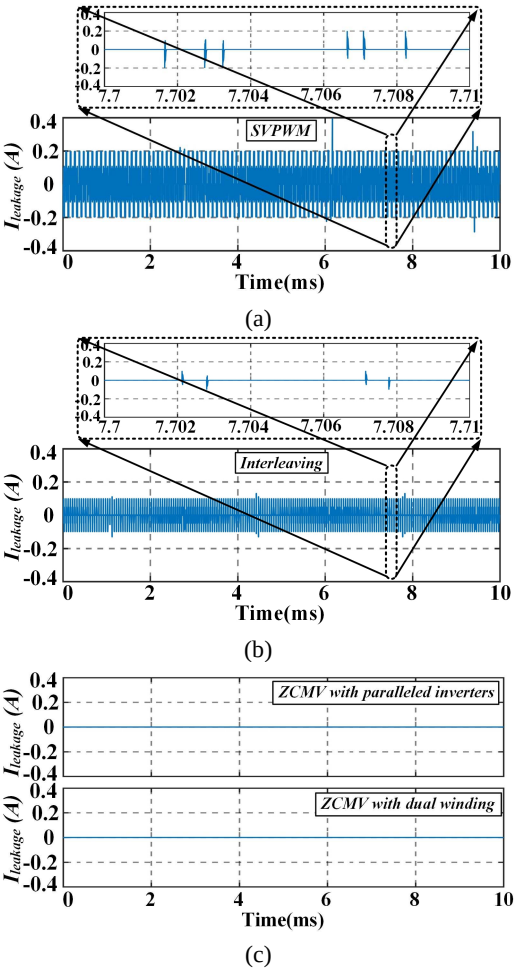

(a)

(b)

(c)

Fig. 17 The leakage current comparison for different schemes: (a) the conventional SVPWM scheme with the proposed structure, (b) the SVPWM with half switching cycle interleaving with the proposed structure, (c) the proposed ZCMV scheme with the conventional and proposed structures

B. The phase current comparison for ZCMV scheme with different structures

For paralleled inverters with ZCMV scheme, the voltage error for two paralleled phase-legs can be balanced in one switching cycle which leads to the suppression of high frequency circulating current [22], so the phase current can be equally divided to two paralleled phase-legs in ideal condition, and the capacity of two paralleled inverters can be fully utilized. In order to verify the characteristic for the proposed scheme, the phase current performance has been tested in steady state with the motor working at 0.375 rated speed (with 50Hz fundamental frequency) and half rated load (4.15Nm). Fig. 18 shows the results of the original and the proposed structures. For paralleled inverter with CI structure shown in Fig. 18(a), the paralleled phase-leg currents i_{a1} and i_{a2} keep the identical phase angle and peak value, the three-phase currents i_{a1}, i_{b1}, i_{c1} in one inverter also keep symmetrical which means the capacity of one inverter can be fully utilized and the power distribution for paralleled inverters is balanced. In addition, the current ripple of i_{a2} is with half switching cycle phase-shift comparing to i_{a1} owing to the same phase-shift in PWM signal shown in the enlarged view. Fig. 18(b) shows the three phase currents in one set stator winding and the corresponding phase A current in the other stator winding for the proposed dual inverter with dual winding structure. It can be seen that the corresponding phase current can also keep balance and the three-phase currents are also symmetrical which is similar with the situation of paralleled inverter with CI. The only difference is the current ripple variation which is affected by the change of circuit structure. So the proposed dual inverter with dual winding structure has no influence on the capacity of inverter, and the dual stator winding can share the same load in ideal condition.

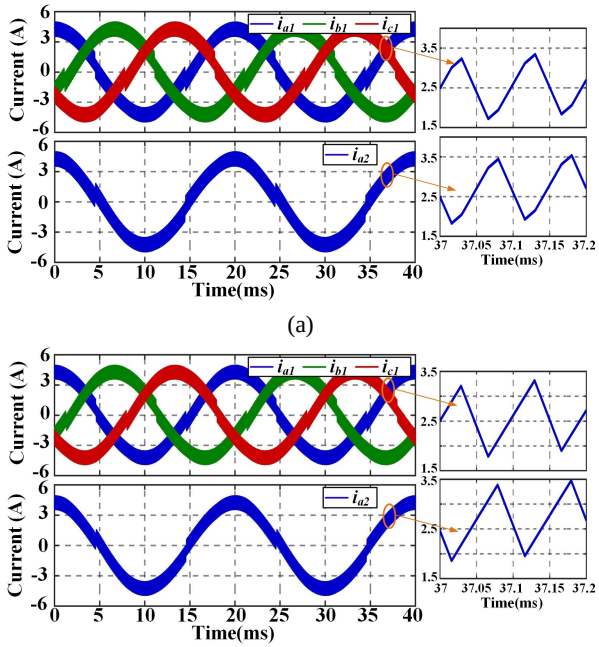

(a)

(b)

Fig. 18 The phase-leg current for different schemes: (a) the phase-leg current for the original paralleled inverters with CI structure, (b) the phase-leg current for the proposed dual inverter with dual winding structure

So from above simulation results, it can be found that, the proposed ZCMV scheme with dual winding structure is feasible in leakage current suppression and has similar performance comparing to the original structure, while the CI can be cancelled in this condition.

V. EXPERIMENTAL RESULTS AND DISCUSSION

In order to further verify the proposed method and compare with other schemes, experiments have been done in a prototype experimental platform shown in Fig. 19, including the motor test bench shown in Fig. 12. The platform consists of a control board, which the control algorithm is implemented in a DSP TMS320F28335 which can generate twelve PWMs and drive two inverter simultaneously, a power board with two integrated power modules (IPM: 6MBP20RH060, 600 V, 20 A, FUJI) connecting the common DC bus which can use as three-phase paralleled inverters or dual separated three-phase inverter. The platform also provide three CIs for paralleled inverter output connection shown in the Fig. 24 for the scheme two. The oscilloscope Rohde & Schwarz RTE1024 with 5GSa/s sampling rate is utilized to capture the date and make sure the precision of time domain waveform. The two line impedance stabilization networks (LISNs: NNBM 8126 A890, 0.1-150MHz, 600V, 100A) are in series with DC power and the inverters to isolated DC power noise. With EMI receiver

Rohde-Schwarz ESL 3 utilized, the CM EMI test can be carried out to get accurate frequency spectrum characteristic. The copper sheet is utilized to provide common grounding. Other related equipment are used to provide the DC power and add braking torque. The common parameters in the experiment has been listed in Table. IV.

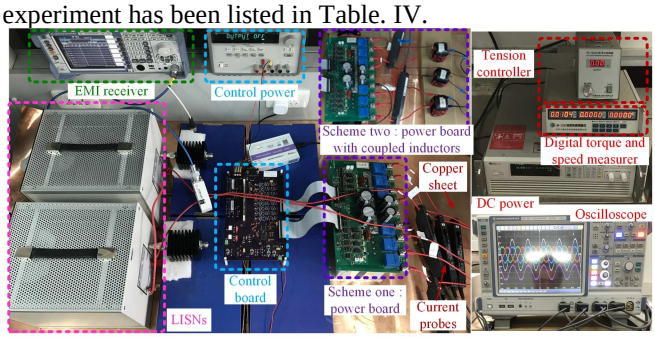

Fig. 19 Experimental platform

TABLE IV. EXPERIMENTAL PARAMETERS

Symbol	Parameters	Value
V_{dc}	DC link voltage	75V
f_s	Switching frequency	10kHz
L_c	Main inductance of CI	0.52mH
M	Coupling coefficient of CI	0.92
L_s	Stator inductance	1.2mH
N_{ref}	Reference rotation speed	375rpm
T_e	Reference torque	4.15Nm
T_d	Dead-time	0.5μs

A. Verification the CMV related motor frame voltage for different schemes

The frame grounding is first cancelled to measure the motor frame voltage in this condition. Based on aforementioned stator winding configurations, the CMV and motor frame voltage of paralleled inverters with CI and the dual inverter with dual winding schemes are tested to verify the feasibility of CI elimination. In this case, three different modulation schemes are implemented, including the conventional SVPWM, the SVPWM with interleaving and the ZCMV. Fig. 20 shows the test results of stator winding CMV, motor frame voltage and the phase-leg current to give the fundamental period reference. For conventional SVPWM utilizing the structure of paralleled inverters with CI and dual inverter with dual winding shown in Fig. 20(a) and (b), the CMV is symmetric six-step wave with the peak value of $\pm V_{dc}/2$ regardless the instantaneous voltage overshoot shown in the enlarged two switching cycles view. More importantly, the motor frame voltage is directly related with the CMV which can be almost recognized as the replica, and only the amplitude is smaller than the CMV. In addition, for the SVPWM with interleaving, the result for the two structures are shown in Fig. 20(c) and (d). It can be found that the CMV in different structures have been reduced to $\pm V_{dc}/6$ which coincide with the theoretical analysis, and the motor frame voltage also keep the replicating relationship with CMV. As for the ZCMV scheme with two structures shown in Fig. 20(e) and (f), the CMV can be further reduced comparing to interleaving manner that only small spikes are left. This spikes are owing to the short dead-time and switching cancellation transient process and so on [19]. Even with some non-ideal factors, the motor frame voltage can also be further reduced which is benefit for the leakage current suppression.

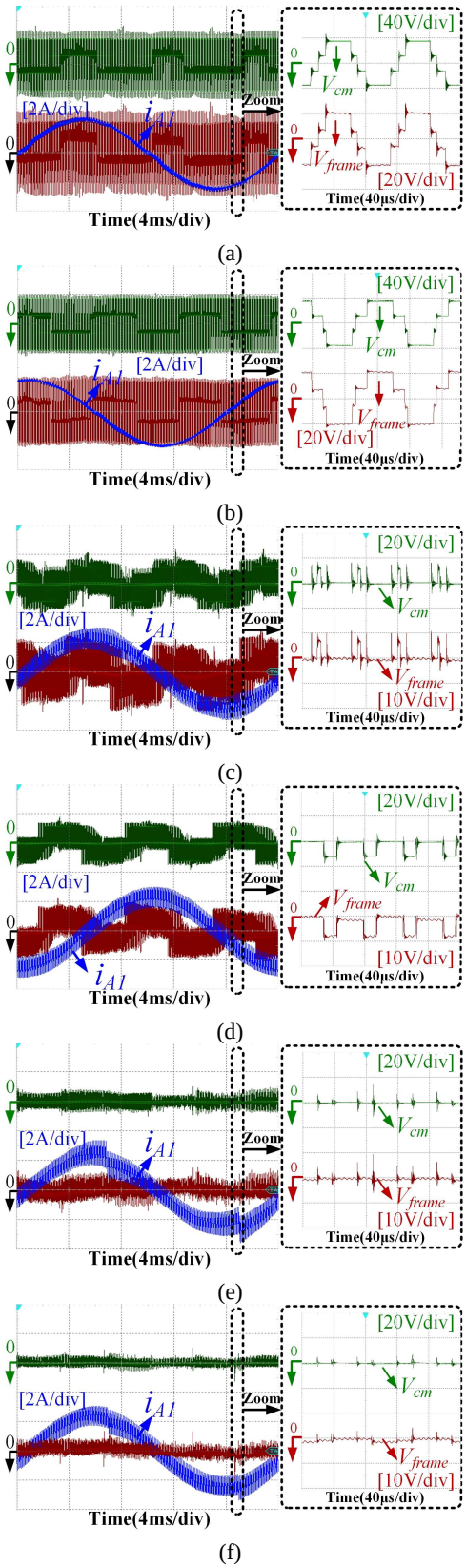

Fig. 20 The CMV, motor frame voltage and phase-leg current comparison for different schemes: (a) the conventional SVPWM for paralleled inverters with CI, (b) the conventional SVPWM for dual inverter with dual winding, (c) the SVPWM for paralleled inverters with CI utilizing interleaving manner, (d) the SVPWM for dual inverter with dual winding utilizing interleaving manner, (e) the ZCMV for paralleled inverters with CI, (f) the ZCMV for dual inverter with dual winding

Considering the above experimental results, it can be concluded that the dual inverter can directly drive the designed two-segment motor without the interference of CMV and motor frame voltage suppression.

B. Comparison of the leakage current and CM EMI for different modulation schemes

In order to further test the CM leakage current and CM EMI with different schemes, the motor frame is connected to the common copper sheet. In this case, Fig. 21 shows the CMC comparison for different structures. In Fig. 21(a), the CMC for three different modulation schemes with conventional structure have been tested. It can be seen that the SVPWM scheme with the largest motor frame voltage leads to about 0.18A peak value of CMC regardless some instantaneous spikes which is the largest CMC in this three schemes. The SVPWM with interleaving scheme which reduces but cannot eliminate the motor frame voltage can suppress the CMC to about 0.1A. The ZCMV scheme which can almost eliminate the motor frame voltage has the best CMC suppression effect and the peak value is less than 0.1A, and the RMS and average value have been reduced which has obvious superiority of EMI reduction. The left CMC is induced by the left frame voltage spike which is caused by the non-ideal factors, such as dead-time effect, the transition process of switching actions, stator inductance asymmetry and so on [19]. More importantly, considering the proposed structure, the CMC result has also been tested shown in Fig. 21(b). It can be seen that the CMC for the three modulation schemes have similar effect with the schemes in conventional structure correspondingly, and the ZCMV scheme also maintain the best CMC suppression effect which proves the feasibility of the proposed scheme.

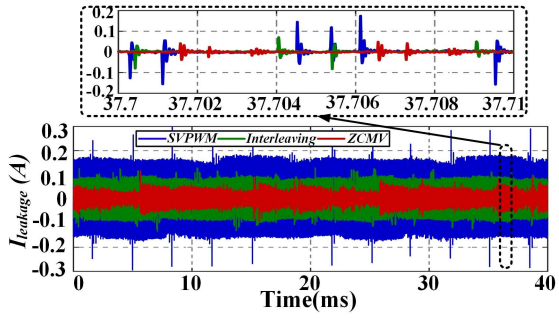

(a)

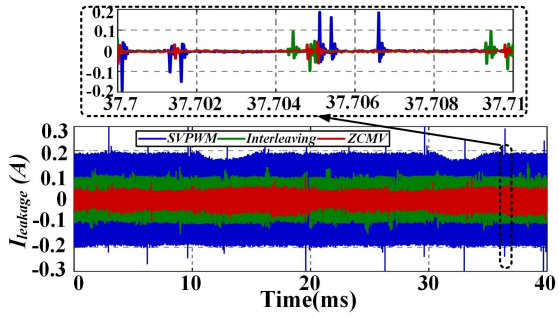

(b)

Fig. 21 The CMC comparison for different schemes: (a) the conventional paralleled inverters with CI structure for three modulation schemes, (b) the proposed dual inverter with dual winding structure for three modulation schemes

In addition, the DC side CM EMI for different schemes have been measured and compared with the EMI standard DO-16050[26] shown in Fig. 22. First, the CM EMI comparison for the three different modulation schemes with conventional structure have been tested and shown in Fig. 22(a). It can be seen that in low EMI frequency range (150 kHz to 1 MHz), the SVPWM with interleaving scheme can restrain the CM EMI near the odd switching frequency comparing to conventional SVPWM scheme which leads to about 10dB EMI peak reduction. Considering the ZCMV scheme, the proposed ZCMV scheme can significantly reduce CM EMI regardless of the odd or even switching frequency and the peak EMI can further reduce about 10dB comparing to SVPWM with interleaving scheme from 150 kHz to 600 kHz. At high EMI frequency range (2 MHz to 30 MHz), the influence of PWM is not dominating, so the three cases are close to each other. So considering the requirement of EMI standard, the ZCMV scheme can help lower the EMI filter cost and component sizes. In Fig. 22(b), the CM EMI comparison for the proposed structure has bene implemented. It can be seen that the characteristic for different modulation schemes in low EMI frequency range keep similar comparing to the conventional structure. While with the change of CM loop impedance caused by the stator winding variation, the CM EMI in high EMI frequency range for the proposed structure has different resonant frequency, but the characteristic of CM EMI in high frequency range cannot obviously affect the EMI filter in this case, so the ZCMV scheme for the proposed structure which has the lowest CM EMI comparing to other modulation schemes can also provide the function of size reduction for CM EMI filter.

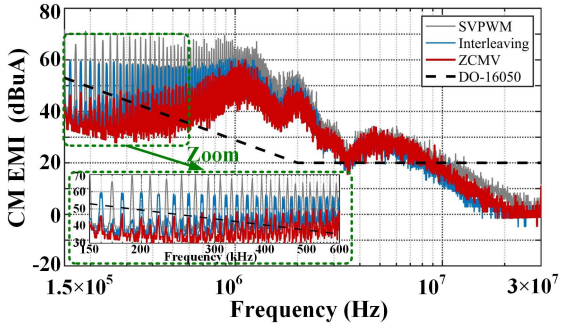

(a)

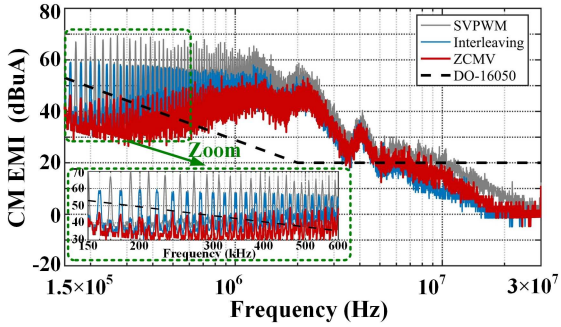

(b)

Fig. 22 The CM EMI comparison for different schemes: (a) the conventional paralleled inverters with CI structure for three modulation schemes, (b) the proposed dual inverter with dual winding structure for three modulation schemes

C. Comparison of the phase current for different schemes

Finally, the steady state experiment has been carried out with the motor working at 0.375 rated speed (with 50Hz

fundamental frequency) and 0.5 rated load (4.15Nm), and the performance of the proposed structure with ZCMV scheme has been tested and compared with the conventional structure. The AC side phase-leg currents have been measured shown in Fig. 23. Fig. 23(a) shows the ZCMV scheme utilizing paralleled inverter with CI structure, in which i_{A1}, i_{B1}, i_{C1} are the three phase-leg currents for one inverter, i_{A2} is the other paralleled phase-leg current for phase A, and i_A is the actual phase A current which is the summation of i_{A1} and i_{A2}. It can be found that owing to the ZCMV scheme, the fundamental phase current can be evenly distributed to paralleled phase-legs. Considering the current ripple shown in the enlarge view, the current ripple of i_{A2} is with half switching cycle phase-shift comparing to i_{A1} owing to the same phase-shift of PWM signal, and the waveform is similar with simulation result.

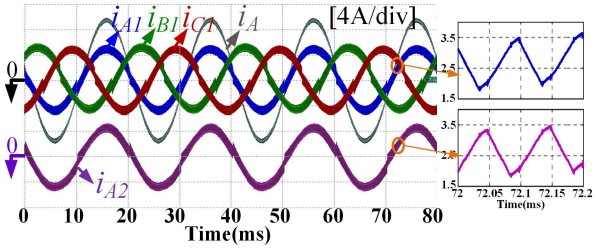

(a)

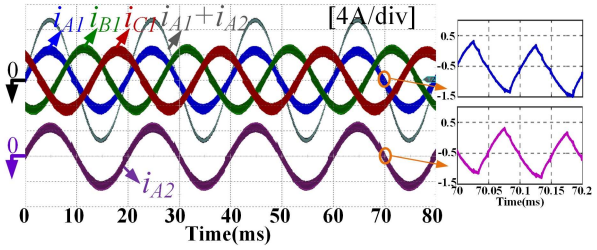

(b)

Fig. 23 The phase current comparison for different schemes: (a) the ZCMV scheme utilizing paralleled inverter with CI structure, (b) the ZCMV scheme for dual inverter with dual winding structure

As for the proposed dual inverter with dual-segment motor, the result is shown in Fig. 23(b), in which i_{A1}, i_{B1}, i_{C1} are the three phase currents for one set stator winding, i_{A2} is the corresponding phase A current for the other stator winding, and $i_{A1}+ i_{A1}$ is the equivalent phase A current. It can be found that the amplitude of corresponding phase currents keep almost identical which is about half of designed rated current for each winding. So the ZCMV scheme can also keep corresponding phase current equally divided in the proposed dual winding structure, and this characteristic ensures the contribution to output torque same for the two set stator windings and make full use of the capacity of the dual inverter system. In addition, with the phase-shift of PWM signal, the current ripple in the corresponding phase current maintain the homologous interleaved effect shown in the enlarge view which also coincides with the simulation result, and this effect makes the equivalent phase A current has similar performance comparing to conventional structure, so it can be easily deduced that the torque ripple caused by the ripple current in phase current will not be degraded in this case.

VI. CONCLUSIONS

In this paper, the complete scheme to deal with the leakage current and CM EMI of motor is proposed. Comparing to the conventional scheme of paralleled inverters with CI to drive three-phase motor, the proposed scheme can directly drive the designed dual-segment three-phase motor which can cancel the utilization of CI and simplify the system structure. Few conclusions can be derived:

1. The ZCMV modulation scheme can cooperate with the specially designed motor to cancel out the CI in motor drive system, and the specially designed motor demand identical two groups of three-phase back-EMF.
2. With the CI cancellation in motor drive system and utilizing ZCMV modulation scheme, the CMV elimination effect can be retained which almost has no influence on leakage current and CM EMI reduction.
3. The proposed ZCMV with dual-segment motor can keep corresponding phase current equally distributed in the dual winding, which makes sure the same contribution to motor output torque and make full use of the capacity of the dual inverter system.

The simulation and experimental results all show that the proposed complete scheme is effective to reduce the leakage current and CM EMI. Compared with the previous work of zero-CM PWM for paralleled inverters, power density of the motor drive can be improved significantly by removing the coupled inductors.

ACKNOWLEDGEMENT

This paper is with support of National Natural Science Foundation of China (NSFC) project 51607077.

REFERENCES

[1] S. Ogasawara and H. Akagi, "Modeling and damping of high-frequency leakage currents in PWM inverter-fed AC motor drive systems," *IEEE Trans. Ind. Appl.*, vol. 32, no. 5, pp. 1105-1114, Sep/Oct 1996.
[2] H. Akagi and T. Shimizu, "Attenuation of conducted EMI emissions from an inverter-driven motor," *IEEE Trans. Power Electron.*, vol. 23, no. 1, pp. 282–290, Jan. 2008.
[3] J. M. Erdman, R. J. Kerkman, D. W. Schlegel and G. L. Skibinski, "Effect of PWM inverters on AC motor bearing currents and shaft voltages," *IEEE Trans. Ind. Appl.*, vol. 32, no. 2, pp. 250-259, Mar/Apr 1996.
[4] D. Busse, J. Erdman, R. J. Kerkman, D. Schlegel, and G. Skibinski, "Bearing currents and their relationship to PWM drives," *IEEE Trans. Power Electron.*, vol. 12, no. 2, pp. 243–252, Mar. 1997.
[5] A.Muetze, "Scaling Issues for Common-Mode Chokes to Mitigate Ground Currents in Inverter-Based Drive Systems," *IEEE Trans. Ind. Appl.*, vol.45, no.1, pp.286-294, Jan.-Feb. 2009.
[6] A. Muetze and C. R. Sullivan, "Simplified design of common-mode chokes for reduction of motor ground currents in inverter drives," *IEEE Trans. Ind. Appl.*, vol. 47, no. 6, pp. 2570–2577, Nov./Dec. 2011.
[7] M. L. Heldwein, L. Dalessandro, and J. W. Kolar, "The three-phase common-mode inductor: Modeling and design issues," *IEEE Trans. Ind. Electron.*, vol. 58, no. 8, pp. 3264–3274, Aug. 2011.
[8] F. Luo, S. Wang, F. Wang, D. Boroyevich, N. Gazel, Y. Kang, and A. C. Baisden, "Analysis of CM volt-second influence on CM inductor saturation and design for input EMI filters in three-phase DC-fed motor drive systems," *IEEE Trans. Power Electron.*, vol. 25, no. 7, pp. 1905–1914, Jul. 2010.
[9] M. Piazza, G. Tine, and G. Vitale, "An improved active common-mode voltage compensation device for induction motor drives," *IEEE Trans. Ind. Electron.* vol. 55, no. 4, pp. 1823–1834, Apr. 2008.
[10] S. Wang, Y. Y. Maillet, F. Wang, D. Boroyevich and R. Burgos, "Investigation of Hybrid EMI Filters for Common-Mode EMI Suppression in a Motor Drive System," *IEEE Trans. Power Electron.*, vol. 25, no. 4, pp. 1034-1045, April 2010.

[11] A. Muetze, "On a new type of inverter-induced bearing current in large drives with one journal bearing," *IEEE Trans. Ind. Appl.*, vol. 46, no. 1, pp. 240–248, Jan./Feb. 2010.
[12] A. M. Hava and E. Ün, "A High-Performance PWM Algorithm for Common-Mode Voltage Reduction in Three-Phase Voltage Source Inverters," *IEEE Trans. Power Electron.*, vol. 26, no. 7, pp. 1998-2008, July 2011.
[13] E. Un and A. M. Hava, "A near-state PWM method with reduced switching losses and reduced common-mode voltage for three-phase voltage source inverters," *IEEE Trans. Ind. Appl.*, vol. 45, no. 2, pp. 782–793, Mar./Apr. 2009.
[14] R. M. Tallam, R. J. Kerkman, D. Leggate, and R. A. Lukaszewski, "Common-mode voltage reduction PWM algorithm for ac drives," *IEEE Trans. Ind. Appl.*, vol. 46, no. 5, pp. 1959–1969, Sep./Oct. 2010.
[15] H. Zhang, A. von Jouanne, S. Dai, A. K. Wallace, and F. Wang, "Multilevel inverter modulation schemes to eliminate common-mode voltages," *IEEE Trans. Ind. Appl.*, vol. 36, no. 6, pp. 1645–1653, Nov./Dec. 2000.
[16] T.-K. T. Nguyen, N.-V. Nguyen, and N. R. Prasad, "Eliminated common mode voltage pulse-width modulation to reduce output current ripple for multilevel inverters," *IEEE Trans. Power Electron.*, vol. 31, no. 8, pp. 5952–5966, Aug. 2016.
[17] A. von Jauanne and H. Zhang, "A dual-bridge inverter approach to eliminating common-mode voltages and bearing and leakage currents," *IEEE Trans. Power Electron.*, vol. 14, no. 1, pp. 43–48, Jan. 1999.
[18] D. Han, C. T. Morris, and B. Sarlioglu, "Common-mode voltage cancellation in PWM motor drives with balanced inverter topology," *IEEE Trans. Ind. Electron.*, vol. 64, no. 4, pp. 2683–2688, Apr. 2017.
[19] D. Han, W. Lee, S. Li and B. Sarlioglu, "New Method for Common Mode Voltage Cancellation in Motor Drives: Concept, Realization, and Asymmetry Influence," *IEEE Trans. Power Electron.*, vol. 33, no. 2, pp. 1188-1201, Feb. 2018.
[20] F. Ueda, K. Matsui, M. Asao, and K. Tsuboi, "Parallel-connections of pulsewidth modulated inverters using current sharing reactors," *IEEE Trans. Power Electron.*, vol. 10, no. 6, pp. 673–679, Nov. 1995.
[21] J. W. Kimball and M. Zawodniok, "Reducing common-mode voltage in three-phase sine-triangle PWM with interleaved carriers," *IEEE Trans. Power Electron.*, vol. 26, no. 8, pp. 1998–2008, Aug. 2011.
[22] D. Jiang, Z. Shen and F. Wang, "Common-mode Voltage Reduction for Paralleled Inverters," *IEEE Trans. Power Electron.*, vol. 33, no. 5, pp. 3961-3974, May 2018.
[23] G. Gohil et al., "Modified discontinuous PWM for size reduction of the circulating current filter in parallel interleaved converters," *IEEE Trans. Power Electron.*, vol. 30, no. 7, pp. 3457–3470, Jul. 2015.
[24] Y. Murai, T. Kubota, and Y. Kawase, "Leakage current reduction for a high-frequency carrier inverter feeding an induction motor," *IEEE Trans. Ind. Appl.*, vol. 28, no. 4, pp. 858–863, Jul./Aug. 1992.
[25] K. Zhou and D. Wang, "Relationship between space-vector modulation and three-phase carrier-based PWM: A comprehensive analysis," *IEEE Trans. Ind. Electron.*, vol. 49, no. 1, pp. 186–196, Feb. 2002.
[26] Environmental Conditions and Test Procedures for Airborne Equipment, DO-160E, RTCA, Inc., Washington, DC, 2004.

Zewei Shen (S'17) was born in Hubei, China, in 1990. He received the B.S. degree in automation from the Department of Automation, Huazhong University of Science and Technology, Wuhan, China, in 2012. He is currently working toward the Ph.D. degree in electrical engineering at Huazhong University of Science and Technology, Wuhan, China.
His current research interests include paralleled converters and high power density motor drive.

Dong Jiang (S05'-M12'-SM16') received B.S and M.S degrees in Electrical Engineering from Tsinghua University, Beijing, China, in 2005 and 2007 respectively. He began his PhD study in Center for Power Electronics Systems (CPES) in Virginia Tech in 2007 and was transferred to University of Tennessee with his advisor in 2010. He received his PhD degree in University of Tennessee in Dec. 2011. He was with United Technologies Research Center (UTRC) in Connecticut as a Senior Research Scientist/Engineer from Jan 2012 to July 2015. He has been with Huazhong University of Science and Technology (HUST) in China as a professor since July 2015. Dong Jiang's major research area is power electronics and motor drives, with more than 40 published IEEE journal and conference papers in this area. He has two best paper awards in IEEE conferences. He is an associate editor of IEEE Transactions on Industry Applications.

Tianjie Zou (S' 15) was born in Hubei, China in 1991. He received the B.E.E. degree in electrical and electronic engineering, from Huazhong University of Science and Technology, Wuhan, China, in 2013, where he is currently working towards his Ph.D. degree in electrical engineering. His main research interests include design, analysis and intelligent control of permanent-magnet machines.

Ronghai Qu (S'01–M'02–SM'05–F'18) was born in China. He received the B.E.E. and M.S.E.E. degrees in electrical engineering from Tsinghua University, Beijing, China, in 1993 and1996, respectively, and the Ph.D. degree in electrical engineering from the University of Wisconsin-Madison, in 2002. In 1998, he joined the Wisconsin Electric Machines and Power Electronics Consortiums as Research Assistant. He became a Senior Electrical Engineer with Northland, a Scott Fetzer Company in 2002. Since2003, he had been with the General Electric (GE) Global Research Center, Niskayuna, NY, as a Senior Electrical Engineer with the Electrical Machines and Drives Laboratory. He has authored over 50 published technical papers and is the holder of over 40 patents/patent applications. From 2010, he has been a professor with Huazhong University of Science &Technology, Wuhan, China. Prof. Qu is a full member of Sigma Xi. He has been the recipient of several awards from GE Global Research Center since 2003, including the Technical Achievement and Management Awards. He also is the recipient of the 2003 and 2005 Best Paper Awards, third prize, from the Electric Machines Committee of the IEEE Industry Applications Society at the 2002 and2004 IAS Annual Meeting, respectively.